

## JOINT TIME-FREQUENCY AND WAVELET ANALYSIS - AN INTRODUCTION

**Andrzej Majkowski, Marcin Kołodziej, Remigiusz J. Rak**

*Warsaw University of Technology, Institute of the Theory of Electrical Engineering, Measurement and Information Systems, Koszykowa 75, 00-662 Warsaw, Poland, (✉ remigiusz.rak@ee.pw.edu.pl)*

### Abstract

A traditional frequency analysis is not appropriate for observation of properties of non-stationary signals. This stems from the fact that the time resolution is not defined in the Fourier spectrum. Thus, there is a need for methods implementing joint time-frequency analysis (t/f) algorithms. Practical aspects of some representative methods of time-frequency analysis, including Short Time Fourier Transform, Gabor Transform, Wigner-Ville Transform and Cone-Shaped Transform are described in this paper. Unfortunately, there is no correlation between the width of the time-frequency window and its frequency content in the t/f analysis. This property is not valid in the case of a wavelet transform. A wavelet is a wave-like oscillation, which forms its own “wavelet window”. Compression of the wavelet narrows the window, and vice versa. Individual wavelet functions are well localized in time and simultaneously in scale (the equivalent of frequency). The wavelet analysis owes its effectiveness to the pyramid algorithm described by Mallat, which enables fast decomposition of a signal into wavelet components.

Keywords: frequency analysis, time-frequency analysis, Short-Time Fourier Transform, Gabor Transform, Wigner-Ville Transform, Cone-Shaped Transform, wavelet analysis, time-scale analysis, wavelet decomposition, filter banks, wavelet packets.

© 2014 Polish Academy of Sciences. All rights reserved

### 1. Introduction

The instrumentation and measurement (I&M) is used in many different fields of technology. It should keep up with the progress in many other modern and fast growing areas. It seems that the most significant among them are information and communication technologies (ICT) and digital signal processing (DSP). Computer engineering with its latest advances enables practical use of advanced signal processing algorithms in real time.

It should be noted that the traditional frequency analysis is not suitable for observing the properties of non-stationary signals. In that case, a joint analysis in time and frequency is required (JFTA - Joint Time-Frequency Analysis). The time-frequency (t/f) analysis enables simultaneous observation of signal properties both in time and in frequency domains. The main shortcoming of the t/f analysis is that there is no correlation between the width of the time-frequency window and its frequency content. Furthermore, this content is always fixed in terms of a signal shape. It is a sinewave [1–2].

The wavelet analysis is devoided of both of these drawbacks. Unlike in the case of a sine waveform, which define the basis for the Fourier transform, the set of wavelet forms is unlimited. Which wavelet is the best, depends on intended application. The most specific feature of the wavelet transform is that individual wavelet functions are well localized in time (or space - for images) and in scale (compressing or stretching a time-limited wavelet) [3]. Wavelets can have a different time compactness as well as shape smoothness [4]. The resulting ability of wavelets to describe a “signal with discontinuities”, with a limited number of

coefficients and with good location in time, is their most meaningful advantage over the time-frequency transforms.

Wavelets owe their remarkable performance, and also their popularity in the signal analysis, to an algorithm described by Mallat in 1989, called the Mallat pyramid [5]. This algorithm is used to obtain the decomposition of the measured signal into wavelet components, using so called quadrature mirror filters.

## 2. Short-Time Fourier Transform

The Short-Time Fourier Transform (STFT) is a typical algorithm of the time-frequency ( $t/f$ ) analysis [1,6,7]. It allows extracting the information of how the signal spectrum changes over time. The analyzed signal, with the help of a sliding time window  $\varphi(t)$ , is divided into blocks (which may overlap). The effect of the sliding time window, with its location described by the  $\tau$  parameter, is described by the formula (1).

$$x_{\tau}(t) = x(t)\varphi(t - \tau). \quad (1)$$

Each signal block is subject to the spectral analysis independently. As in the conventional Fourier analysis, time windows of different shapes are used to remove abrupt changes (cuts) of the signal at both ends of the block. Next, the spectral content of the signal is examined.

Two basic normalized parameters are defined for time windows  $\varphi(t)$  [8]: the center (the center of gravity)  $\bar{V}_t$  and the radius (analog of width)  $\Delta_t$ , both measured in terms of the mean square value. In a similar way, the parameters of the window are defined in the frequency domain -  $\bar{V}_{\omega}$  and  $\Delta_{\omega}$ , respectively.

The product of the normalized width of the window in the time domain and the normalized width of the window in the frequency domain is constant for a given window. Thus, improving the resolution in the time domain degrades the resolution in the frequency domain, and vice versa. So, selecting a window width is always a compromise.

According to the uncertainty principle [9]:

$$\Delta_t \Delta_{\omega} \geq \frac{1}{2}. \quad (2)$$

For example, for a rectangular window (with the width of  $2\varepsilon$ ) parameters  $\Delta_t$  and  $\Delta_{\omega}$  take the values:

$$\Delta_t = \frac{\varepsilon}{\sqrt{3}}, \quad \Delta_{\omega} = \infty. \quad (3)$$

So, it is the ideal time window and the worst, unacceptable frequency window for the  $t/f$  analysis.

In light of the foregoing, STFT of the signal  $x(t)$ , with respect to the window  $\varphi(t)$  put in the position  $(\tau, \xi)$  in the  $t/f$  plane, where  $\tau$  - denotes the position on time axis, and  $\xi$  - on  $\omega$  axis, can be defined as:

$$X(\tau, \xi) = \int_{-\infty}^{+\infty} x(t)\varphi(t - \tau)e^{-j\xi t} dt. \quad (4)$$

In the traditional Fourier transform, the calculation of a single component requires knowledge of the function  $x(t)$  along the entire processed block of signal. In the case of STFT, knowledge of  $x(t)$  is required only within the range specified by the position of the window  $\varphi(t-\tau)$ .

The interpretation of the t/f window position on the t/f plane is shown in Fig. 1.

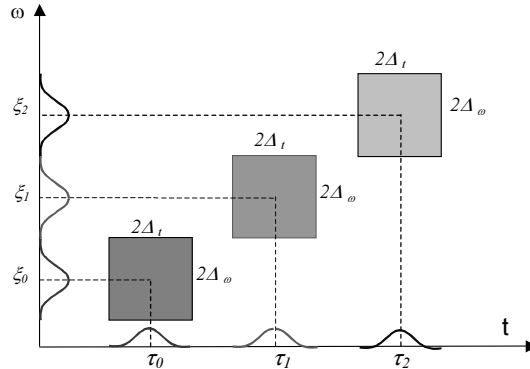


Fig. 1. A window's location across the t/f plane.

Traditionally, a shifted window  $\varphi(t-\tau)$  is considered together with  $x(t)$  - visualized in  $\{\}$  braces in the expression (5). The product  $x(t)\varphi(t-\tau)$ , as a windowed signal, is subject to the traditional Fourier transform:

$$X(\tau, \xi) = \int_{-\infty}^{+\infty} \{x(t)\varphi(t-\tau)\} e^{-j\xi t} dt = \langle x(t)\varphi(t-\tau), e^{j\xi t} \rangle. \quad (5)$$

But, if the factor  $\varphi(t-\tau)$  is considered together with  $e^{j\xi t}$  instead of  $x(t)$ , like in the expression (6) - visualized in  $\{\}$  braces, it can be said that the sliding window  $\varphi(t-\tau)$  is used to modulate the amplitude of the sine wave  $e^{j\xi t}$ . Then, the expression describing STFT looks like:

$$X(\tau, \xi) = \int_{-\infty}^{+\infty} x(t) \{\varphi(t-\tau)e^{-j\xi t}\} dt = \langle x(t), \varphi^*(t-\tau)e^{j\xi t} \rangle = \langle x(t), \varphi_{\tau, \xi}(t) \rangle. \quad (6)$$

And the function:

$$\varphi_{\tau, \xi}(t) = \varphi(t-\tau)^* e^{j\xi t}. \quad (7)$$

behaves like a package of sine waves oscillating inside the window  $\varphi(t)$ . This package may be considered as a set of new basis functions for STFT, which are limited in time as well as in frequency. This approach allows to treat STFT as an algorithm that decomposes  $x(t)$  into the components of the base defined by equation (7).

The discrete version of the equation (4) becomes (8):

$$X(\tau_n, \xi_k) = T_p \sum_{i=0}^{N-1} x(t_i)\varphi(t_i - \tau_n)e^{-j\xi_k t_i}. \quad (8)$$

where  $T_p$  is the sampling period. For normalization, when  $T_p=1$ :

$$X_{n,k} = \sum_{i=0}^{N-1} x(i)\varphi(i-n)e^{-j2\pi ki/N}. \quad (9)$$

Based on STFT, a spectrogram may be determined which is a signal energy representation:  $SPEC [X_{n,k}] = |X_{n,k}|^2$ .

Fig. 2 shows an example of the STFT analysis (with two different widths of the time window). The examined signal, sampled with the frequency of 1000Hz, consists of two parts (time intervals: 0.10-0.15s and 0.25-0.58s). The first part is a sinusoidal signal with the frequency of 312Hz, the second part is a superposition of two signals: the sine-wave with the frequency of 84Hz and the sine-wave with the frequency modulated linearly in the range of 180-400Hz. The original waveform is shown at the bottom of each part. The right part of the illustrations shows the power spectrum of the signal.

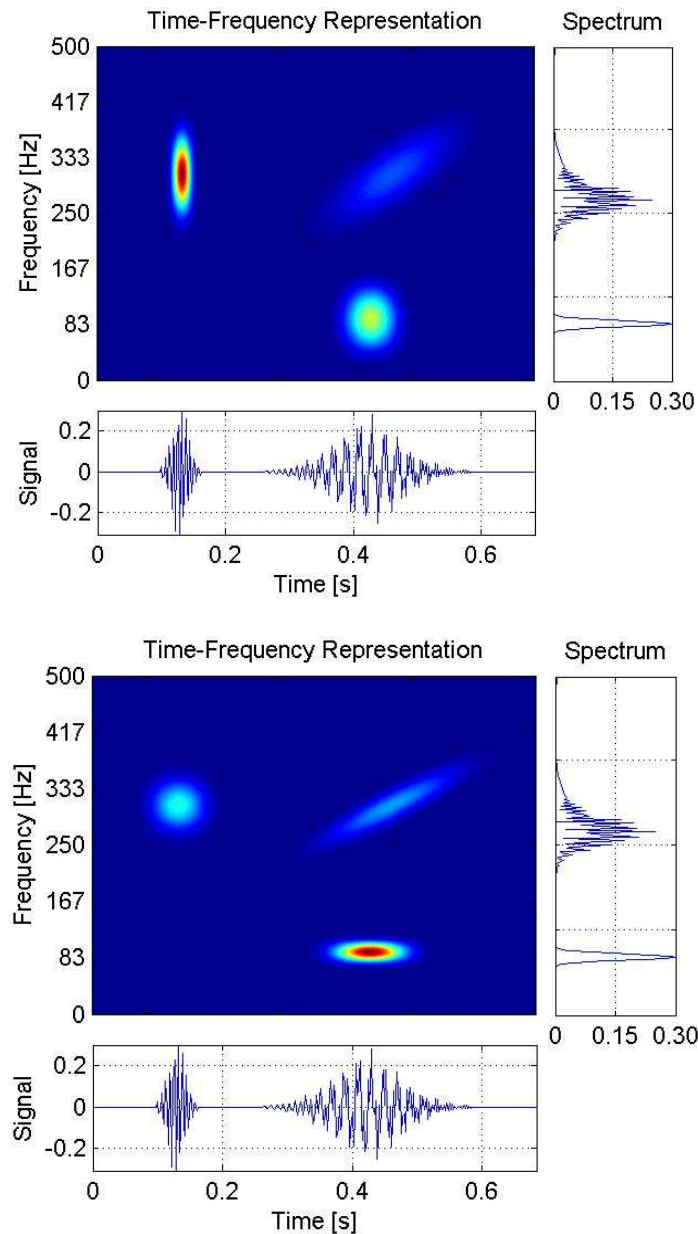


Fig. 2. A practical example of the STFT decomposition for a narrow time window (top part: Hanning, 32 samples) and a wide time window (bottom part: Hanning, 128 samples).

Analyzing the traditional signal spectrum it may be determined which frequency components of the signal are present, but nothing could be said about the moments of their presence. It is also difficult to determine the nature of signal changes in frequency. However, by observing

the signal decomposition in the t/f plane, we can determine both the moments of occurrence of a specific signal components and the nature of their changes in frequency.

Unfortunately, STFT signal decomposition in time and frequency can be determined only with a certain limited precision, defined by the window parameters. Usage of a narrow time window (and thus wide in the frequency domain) results in a bad location in the frequency domain and a relatively good resolution in time (Fig. 2 top). The use of a wide time window (Fig. 2 bottom) gives a good location in frequency and poor location in time.

### 3. Gabor transform

There is a special case of the t/f analysis (10), in which the time window has a specific, Gaussian shape. It turns out that the spectrum of this window also has the Gaussian shape.

$$\varphi(t) = g(t) = \frac{1}{2\pi\alpha} e^{-t^2/4\alpha}, \quad \Phi(\omega) = G(\omega) = e^{-\alpha\omega^2}, \quad \alpha > 0. \quad (10)$$

This case meets the conditions of a time-frequency window with the following normalized parameters: *the time window*:  $\nabla_t = 0$ ,  $\Delta_t = \sqrt{\alpha}$ , *the frequency window*:  $\nabla_\omega = 0$ ,  $\Delta_\omega = \frac{1}{2\sqrt{\alpha}}$ .

That window is called the Gabor window after its inventor. The measure of quality of a Gabor window is the product of:  $\Delta_t \Delta_\omega = \frac{1}{2}$ , which reaches the lower limit of the uncertainty principle. The analytical notation of the Gabor transform is presented by (11):

$$G(\tau, \xi) = \int_{-\infty}^{+\infty} x(t) g(t - \tau) e^{-j\xi t} dt. \quad (11)$$

For the purpose of numerical calculations a concept of the discrete Gabor transform defined for a finite set of points in the t/f plane was introduced. A discretized version of the Gabor transform, for a continuous signal  $x(t)$ , in terms of the window position across the t/f plane, (when changes:  $\tau \rightarrow \tau_n$ ,  $\xi \rightarrow \xi_k$  take place) is described by (12):

$$G(\tau_n, \xi_k) = \int_{-\infty}^{+\infty} x(t) g(t - \tau_n) e^{-j\xi_k t} dt. \quad (12)$$

A continuous signal  $x(t)$  may be reconstructed according to the equation known as the Gabor decomposition, similar to the Fourier series [9]:

$$x(t) = \sum_n \sum_k G(\tau_n, \xi_k) g(t - \tau_n) e^{j\xi_k t}. \quad (13)$$

In this case, there is a package of sine-waves modulated by the Gaussian window  $g(t)$ . That package is called the Gabor decomposition base, which due to the Gaussian shape of the window with a minimal size across the t/f plane, is considered to be optimal in terms of signal decomposition and reconstruction.

A practical algorithm for computing the discrete Gabor decomposition has the form [10]:

$$x(i) = \sum_n \sum_{k=0}^{N-1} G_{n,k} g^*(i-n) e^{\frac{j2\pi ki}{N}}. \quad (14)$$

Gabor decomposition coefficients  $G_{n,k}$  are determined by the STFT algorithm according to the equation [10]:

$$G_{n,k} = \sum_{i=0}^{N-1} x(i) g^*(i-n) e^{\frac{-j2\pi ki}{N}}. \quad (15)$$

Fig. 3 shows the results of the t/f analysis using the Gabor transform of the same signal described above for the STFT decomposition.

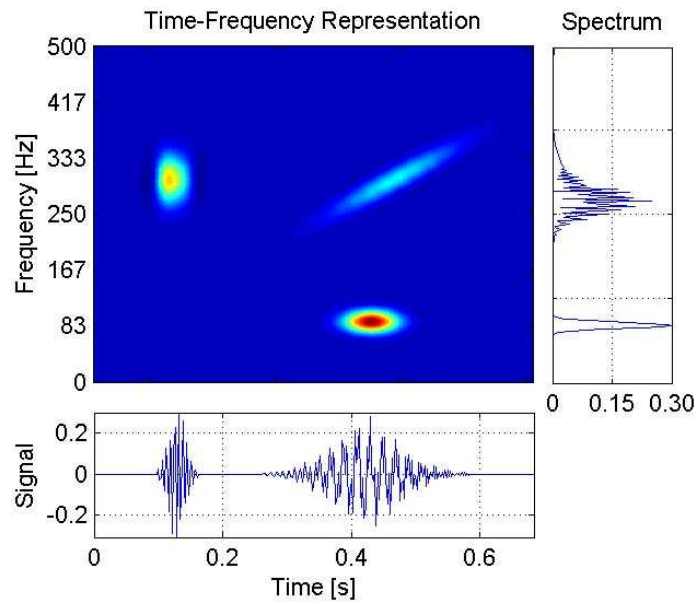


Fig. 3. The result of the time-frequency analysis using the Gabor transform (Gaussian window, 64 samples).

#### 4. Wigner-Ville Transform

The transforms described above do not provide direct information about the signal energy but only about its amplitude. Of course, there is a possibility of determining the energy spectrum by simply squaring obtained spectral components. However, it would be more convenient to define the transform as:

$$X(t, \omega) = \int_{-\infty}^{+\infty} |x(\tau - t)|^2 e^{-j\omega\tau} d\tau = \int_{-\infty}^{+\infty} x(\tau - t) x^*(\tau - t) e^{-j\omega\tau} d\tau. \quad (16)$$

Next, rather than to calculate the value of energy at a certain point in time, it would be better to calculate it in a finite, symmetrical time interval  $(t - \tau/2, t + \tau/2)$ , placed in the neighborhood of  $t$  moment. This requirement formed the basis of the definition of the Wigner-Ville transform (17).

$$WV(t, \omega) = \int_{-\infty}^{+\infty} x\left(t + \frac{\tau}{2}\right) x^*\left(t - \frac{\tau}{2}\right) e^{-j\omega\tau} d\tau. \quad (17)$$

It should be stressed that the Wigner-Ville transform describes a non-linear signal decomposition in the  $t/f$  plane.

After discretization, the equation (17) takes the form:

$$WV(n, k) = \sum_{i=-\infty}^{+\infty} x(n+i)x^*(n-i) e^{-j\frac{2\pi k}{L}i}. \quad (18)$$

A practical method of calculating the Wigner-Ville transform for a discrete signal  $x[n]$  is described by the formula (19) [10]:

$$WV(n, k) = \sum_{i=-L/2}^{L/2} \Re[n, i] e^{-j2\pi ki/L}. \quad (19)$$

where  $\Re[n, i]$  denotes a correlation function described as:  $\Re[n, i] = z[n+i]z^*[n-i]$ , and  $z[n]$  is the signal interpolated from  $x[n]$ . The transform may also be calculated from the formula (20) [8]:

$$WV(n, k) = \sum_{i=-L/2}^{L/2} \Im[n, i] e^{j2\pi ki/L}. \quad (20)$$

where:  $\Im[n, i] = X[n+i]X^*[n-i]$  and  $X[n]$  means the Fourier transform of the signal  $x[n]$ . Fig. 4 presents results of analyzing the same above-mentioned signal using the Wigner-Ville transform.

The Wigner-Ville transform has a very high time-frequency resolution. However, for complicated signals, there are clearly visible parasitic interferences between original frequency components (elements 1,2,3 in Fig. 4).

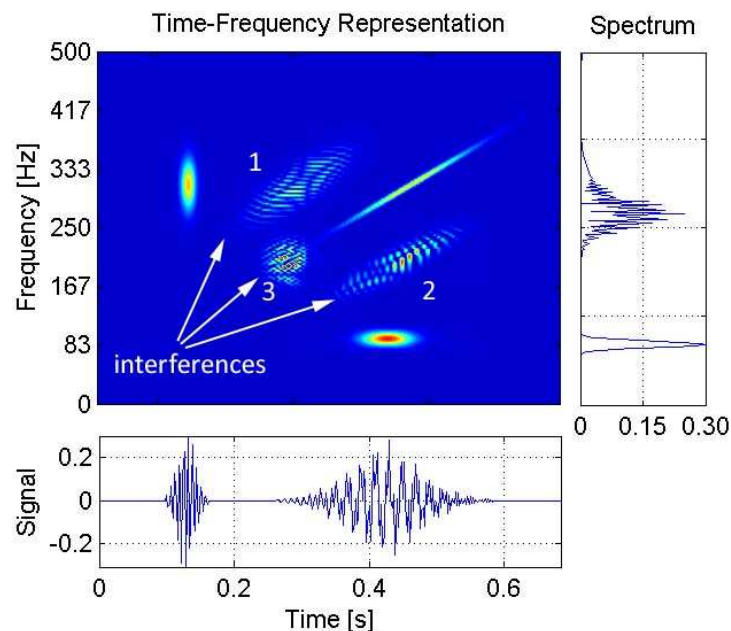


Fig. 4. An example of the  $t/f$  analysis using the Wigner-Ville transform (with interferences).

The Wigner-Ville representation is not linear, so the spectrum of two combined signals is not the sum of their separate spectra, but includes also a cross-spectrum. In a sense, they represent the correlations between each pair of signal components. The individual elements of the signal are described by specifying their duration in time and their frequency range.

Thus, the elements (0.10÷0.15s, 312Hz) and (0.25÷0.58s, 180÷400Hz) generate the interference numbered 1. Elements (0.25÷0.58s, 180÷400Hz) and (0.25÷0.58s, 84Hz) generate the interference numbered 2, and finally elements (0.10÷0.15s, 312Hz) and (0.25÷0.58s, 84Hz) generate the interference denoted by 3. Although the amplitudes of the interferences may reach high values, their mean value is usually limited.

## 5. Choi-Williams transform

An intuitive method of reducing unwanted interferences in the Wigner-Ville transform is to add a kind of filter to it. The result is described by the equation [10]:

$$C_{n,k} = \sum_{i=-L/2}^{L/2} \sum_m K(m,i) \mathfrak{R}[n-m,i] e^{-j2\pi ki/L}, \quad (21)$$

where  $K(m,i)$  is a kernel function. Each transform calculated according to the above formula, belongs to the so called Cohen's class. And when the function  $K(m,i)$  becomes:

$$K(m,i) = \sqrt{\frac{\alpha}{4\pi i^2}} e^{-\alpha m^2 / (4i^2)}, \quad (22)$$

it defines the so called Choi-Williams (CW) transform. The CW transform enables to reduce parasitic interferences while maintaining many useful features of the Wigner-Ville transform. Fig. 5 shows an analysis of the aforementioned signal using the Choi-Williams transform.

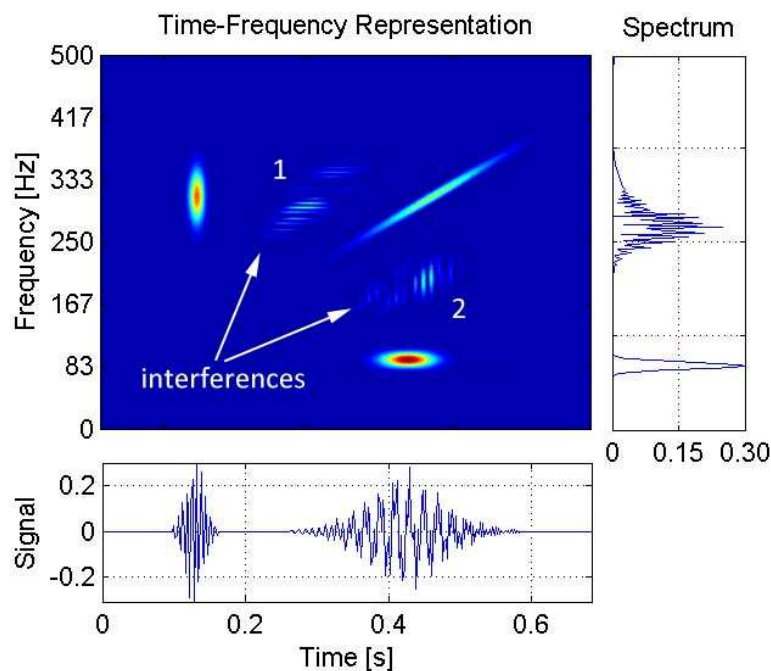


Fig. 5. An illustration of the t/f analysis using the Choi-Williams transform.

This transform can significantly suppress interferences occurring between signal components at different time moments and different frequencies (the case 3 in Fig. 4). Interference between signal components occurring at the same moments or having the same frequency components remain at the same level as for the Wigner-Ville transform. The speed of calculations for the Choi-Williams transform is relatively small.

## 6. Cone-shaped transform

A cone-shaped transform is another approach to reduce the parasitic interferences. Here, in turn, the kernel function is defined as [10]:

$$K(m, i) = \begin{cases} e^{-\frac{\alpha^2}{c}} & \text{for } m \leq |i| \\ 0 & \text{in other cases} \end{cases} \quad (23)$$

The constant  $c$  is usually taken as 500. The level of interferences can be regulated by changing the  $\alpha$  parameter. Unfortunately, reduction of interferences is associated with deterioration of the  $t/f$  resolution.

Fig. 6 presents the results of analyzing the same signal with the Cone-shaped transform. This transform also effectively suppresses type 3 interferences from Fig. 4. There is, however, a quite strong interference between elements of the same frequency or time (number 1 and 2).

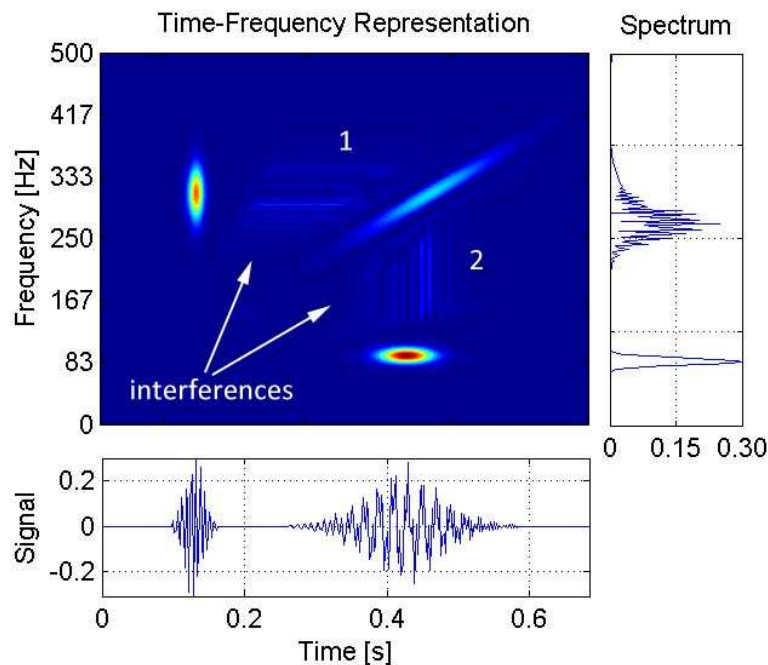


Fig. 6. An illustration of the  $t/f$  analysis using the Cone-shaped transform.

## 7. Continuous wavelet transform

A continuous wavelet transform (CWT) of a function  $x(t) \in L^2(\mathcal{R})$  and a wavelet  $\psi(t)$  is defined as [11,12]:

$$W(\tau, \sigma) = \int_{-\infty}^{+\infty} x(t) \psi_{\tau, \sigma}^*(t) dt, \quad (24)$$

$$\psi_{\tau, \sigma}(t) = \frac{1}{\sqrt{\sigma}} \psi\left(\frac{t - \tau}{\sigma}\right), \quad (25)$$

where  $L^2(\mathcal{R})$  is a one-dimensional vector space of functions which are measurable and integrable in a sense of the mean square,  $\sigma$  is a scale parameter and  $\tau$  a shift. Strictly speaking,

the continuous wavelet transform is described not in the time-frequency ( $t/f$ ) but in the time-scale ( $t/s$ ) space. However, after using a proper transformation the scale can be converted to frequency ( $1/\sigma$  reflects the frequency). The  $\tau$  parameter represents the location of the wavelet along the time axis.

In order to be a *wavelet* and also to enable reconstruction of  $x(t)$ , the function  $\psi(t)$  must be limited in time and satisfy the condition (26) [13,14,15]. In simple terms we can say that *the wavelet must oscillate and fade*.

$$\Psi(\omega)\Big|_{\omega=0} = \int_{-\infty}^{+\infty} \psi(t) e^{-j\omega t} dt = \int_{-\infty}^{+\infty} \psi(t) dt = 0. \quad (26)$$

A wavelet can be considered as a window function similarly to the  $t/f$  window in the STFT. It means that the  $t/f$  window can be replaced by the wavelet (let's refer to it as the wavelet window)  $\psi(t)$  [16]. So, it is possible to define two basic normalized parameters in the time domain: the center  $\nabla_t$  (the center of gravity) and the radius  $\Delta_t$  (analog value of the width), both measured in terms of the mean square value. The parameters of the window in the frequency domain are defined -  $\nabla_\omega$  and  $\Delta_\omega$ , respectively. The transform  $W(\tau, \sigma)$  describes the properties of  $x(t)$  observed in the  $t/f$  window with the ends [9]:

$$[\sigma\nabla_t + \tau - \sigma\Delta_t, \sigma\nabla_t + \tau + \sigma\Delta_t] \times \left[ \frac{1}{\sigma}(\nabla_\omega - \Delta_\omega), \frac{1}{\sigma}(\nabla_\omega + \Delta_\omega) \right]. \quad (27)$$

It should be noted that the product of window radii in the time and frequency domains is constant over the entire  $t/s$  plane [9]:  $2\sigma\Delta_t \frac{2}{\sigma} \Delta_\omega = 4\Delta_t\Delta_\omega$ .

The location of a time-frequency window of the wavelet transform on the  $t/f$  plane (for convenient comparison with the  $t/f$  analysis) is shown in Fig. 7.

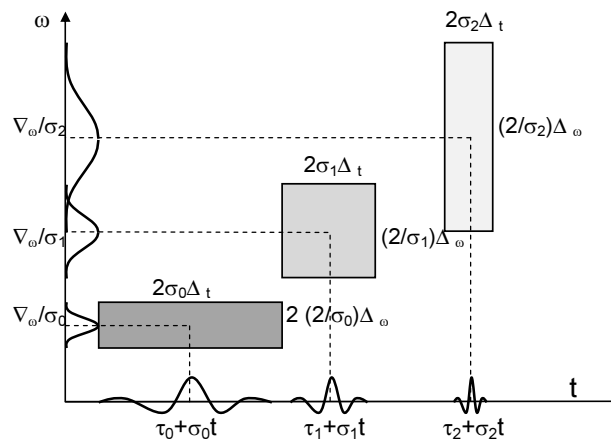


Fig. 7. The location of a wavelet window across the  $t/f$  plane.

It shows clearly that the shape of a wavelet window, which determines the analysis resolution, is a function of the window position on the  $t/s$  plane, in contrast to STFT, where the  $t/f$  resolution is constant across the entire  $t/f$  plane.

The concept of a continuous wavelet transform (CWT) requires the continuous scale and continuous shift in time. Of course, in the context of discrete signals the continuity means changes of single signal samples.

It should be noted that a higher scale of the wavelet analysis is equivalent to a more stretched wavelet. The more stretched a wavelet (higher scale), the larger section of the signal to which it is being compared and the coarser signal features are described.

Rather than being a shortcoming of the method, the fact that the wavelet analysis does not map a signal's features in the  $t/f$  but in the  $t/s$  plane, is its strength. The method proves to be a natural way to describe many physical phenomena perceived by human senses.

## 8. Discrete Wavelet Transform

In order to define a Discrete Wavelet Transform (DWT) the following assumptions are made:

$$\sigma = 2^{-s} \quad \tau = 2^{-s} l, \quad (28)$$

where  $l$  describes the shifting, and  $s$  is the scale factor ( $l = 0, 1, 2, \dots$   $s = 0, 1, 2, \dots$ ). The above formulas combined with the assumption of discretization of  $x(t)$ , produce a new, discrete form of the wavelet transform [9]:

$$\begin{aligned} W(\sigma, \tau) &= W(l2^{-s}, 2^{-s}) = W(l, s) = \\ &= 2^{s/2} \sum_n x(n) \psi(2^s n - l) \end{aligned} \quad (29)$$

It is worth bearing in mind that the wavelet transform does not satisfy the shift invariance condition. Furthermore, the time shift of a function  $x_m(t) = x(t - \tau_m)$  comes in a form of the formula (30) [9].

$$W_{\psi, x}(l, s) = 2^{s/2} \int_{-\infty}^{+\infty} x_m(t) \psi(2^s t - l) dt = W_{\psi, x}((l - m2^s)2^{-s}, 2^{-s}), \quad (30)$$

where indexes  $\psi$  and  $x$  have a symbolic meaning – the wavelet  $\psi(t)$  is used for decomposition of the signal  $x(t)$ .

At this point, one can formulate the expression of a wavelet series, which holds for any function  $x(t) \in L^2(\mathcal{R})$

$$\begin{aligned} \text{where:} \quad x(t) &= \sum_s \sum_l w_{l,s} \psi_{l,s}(t) \\ \psi_{l,s}(t) &= 2^{s/2} \psi(2^s t - l) \end{aligned} \quad (31)$$

If  $\{\psi_{l,s}(t)\}$  forms an orthonormal basis in  $L^2(\mathcal{R})$  space, then similarly as in the case of a Fourier series [5]:

$$w_{l,s} = \langle x(t), \psi_{l,s}(t) \rangle = 2^{s/2} W_{\psi, x}(l, s). \quad (32)$$

The wavelet series is obtained by sampling a continuous wavelet transform across the  $t/s$  plane, at certain dyadic points  $(l2^{-s}, 2^{-s})$ . Should the base  $\{\psi_{l,s}(t)\}$  not satisfy the orthonormal condition,

the analysis becomes more difficult. If that is the case, the so-called dual wavelets as well as the formula for bases  $\{\psi^{A,s}(t)\}$  need to be defined [17].

### 9. Mallat's wavelet decomposition algorithm - Mallat pyramid

A very effective method of implementing the DWT algorithm based on filtering was described in 1989 by Mallat [5]. It refers to the method of “encoding in subbands”, known earlier from the frequency analysis. Two new concepts were introduced to the wavelet analysis: an approximation and a detail. The term “approximation” describes the low-frequency signal components. The “detail” describes the high frequency components. The aforementioned filtering process includes two filters: a low-pass (G) filter and a high-pass (H) one. The low-pass filter separates the approximation of the analyzed signal and the high-pass one the detail of the signal. The complete process of decomposition involves a number of such modules forming the so called wavelet decomposition tree. An example of such a tree is given in Fig. 8.

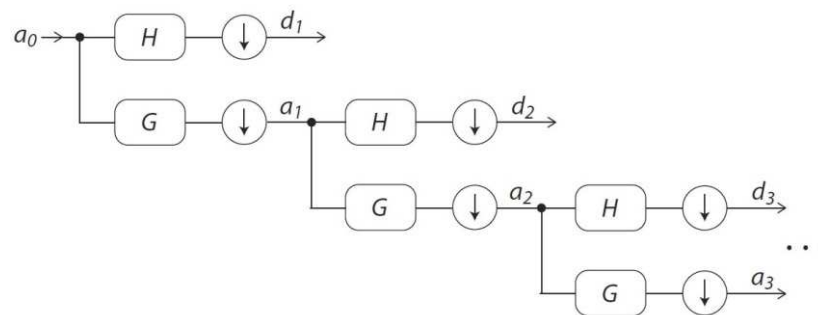


Fig. 8. A wavelet decomposition tree:  $a_0$  - the original signal,  $d_i$  - the detail in the  $i$ -th scale,  $a_i$  - the approximation in the  $i$ -th scale.

According to Fig. 8, the original signal  $a_0$  passes through a pair of complementary filters which divide it into two components:  $a_1$  (approximation) and  $d_1$  (detail).

An example of a one-level wavelet decomposition of a real measurement signal is given in Fig. 9.

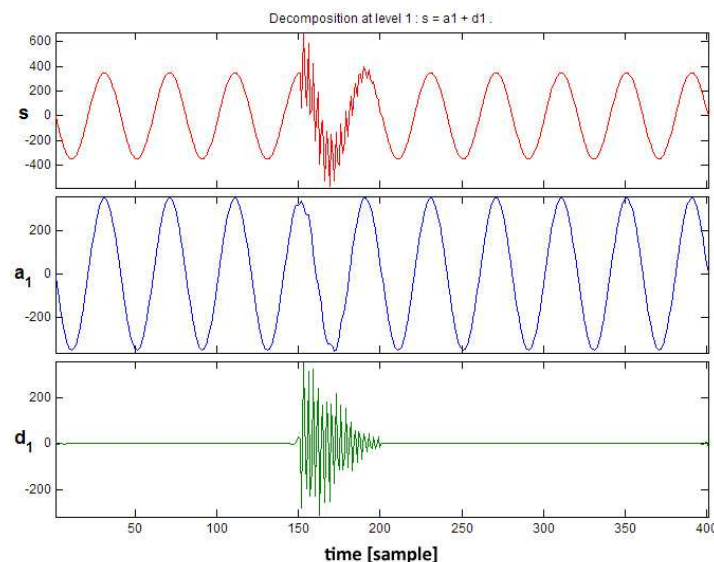


Fig. 9. The effect of a one-level wavelet decomposition.

From the metrological point of view, one could narrow down the discussion about wavelets to the decomposition process, also known as the analysis process. However, it is often necessary

to reconstruct the original signal, as in the signal compression. This process is referred to as a signal reconstruction or synthesis.

The original digital signal can be reconstructed using an algorithm similar to the pyramid analysis. A single step of the reconstruction process is illustrated in Fig. 10. The original digital signal with a resolution of 1, is obtained by repeating this procedure  $J$  times, where  $J$  is the number of levels of the wavelet decomposition.

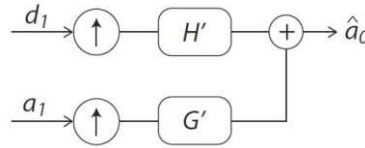


Fig. 10. Reconstruction of the digital approximation of  $\hat{a}_0$  from  $a_1$  in a lower resolution and the detail  $d_1$ .

Filters used for the wavelet decomposition are determined by a chosen wavelet (its shape). Strictly speaking, the shape of a wavelet  $\psi(t)$  is closely related to the high-pass filter that extracts details in the wavelet decomposition.

There is one more, very characteristic function, associated with wavelet sets. It is a so called scaling function, denoted by  $\varphi(t)$ . Its shape is related to the transfer function of low-pass filter responsible for separation of approximation. The shape of the scaling function is similar to the shape of the corresponding wavelet, except that it contains a DC component. The scaling function is defined by a recursive mathematical notation, using the dilation equation [5]:

$$\varphi(t) = \sum_{k=0}^{N-1} h_k \varphi(2t - k). \quad (33)$$

In the context of the scaling function, a wavelet is defined by the same dilation equation, but described by a different set of coefficients:

$$\psi(t) = \sum_{k=0}^{N-1} g_k \varphi(2t - k). \quad (34)$$

The coefficients  $\{h_k\}$  and  $\{g_k\}$  define a couple of quadrature mirror filters. In the case of orthonormal base they are related to the mathematical formula  $g_k = (-1)^k h_{N-k}$ .

## 10. Examples of Wavelets

There is an almost unlimited number of valid wavelets which could be created, as well as so called filter banks [18]. Finding the best one depends on intended implementation. The names of wavelets usually come from their shapes or the names of people who used them for the first time and published the results. Some of wavelet names are: Daubechies, Haar, Coiflets, Symlet, Spline, Battle-Lemarie.

Some properties of wavelets can affect the quality of analysis. These properties are [19]:

- the operating range of the scaling function, the mother wavelet and their Fourier transforms that determines location properties in time and frequency domains;
- the symmetry - which is the condition for avoiding a phase distortion;
- the number of statistical moments identically equal to zero - which determines the quality of potential signal compression;
- the regularity - which determines to some extent a smooth representation of the data;
- the orthogonality or bi-orthogonality;

- the existence of an explicit description;
- the existence of a scaling function.

The variety of wavelet functions is very high. For example, Daubechies wavelet functions do not have explicit description. The basis for their definition is a scaling function  $\varphi(t)$  and a corresponding mother wavelet function  $\psi(t)$ .

Daubechies wavelet functions of N-th order have N vanishing moments (equal to zero). The support of the function is equal to  $(2N-1)$  unbalanced orthogonal functions. Examples of Daubechies wavelet functions and their spectra are shown in Fig. 11 [20,21].

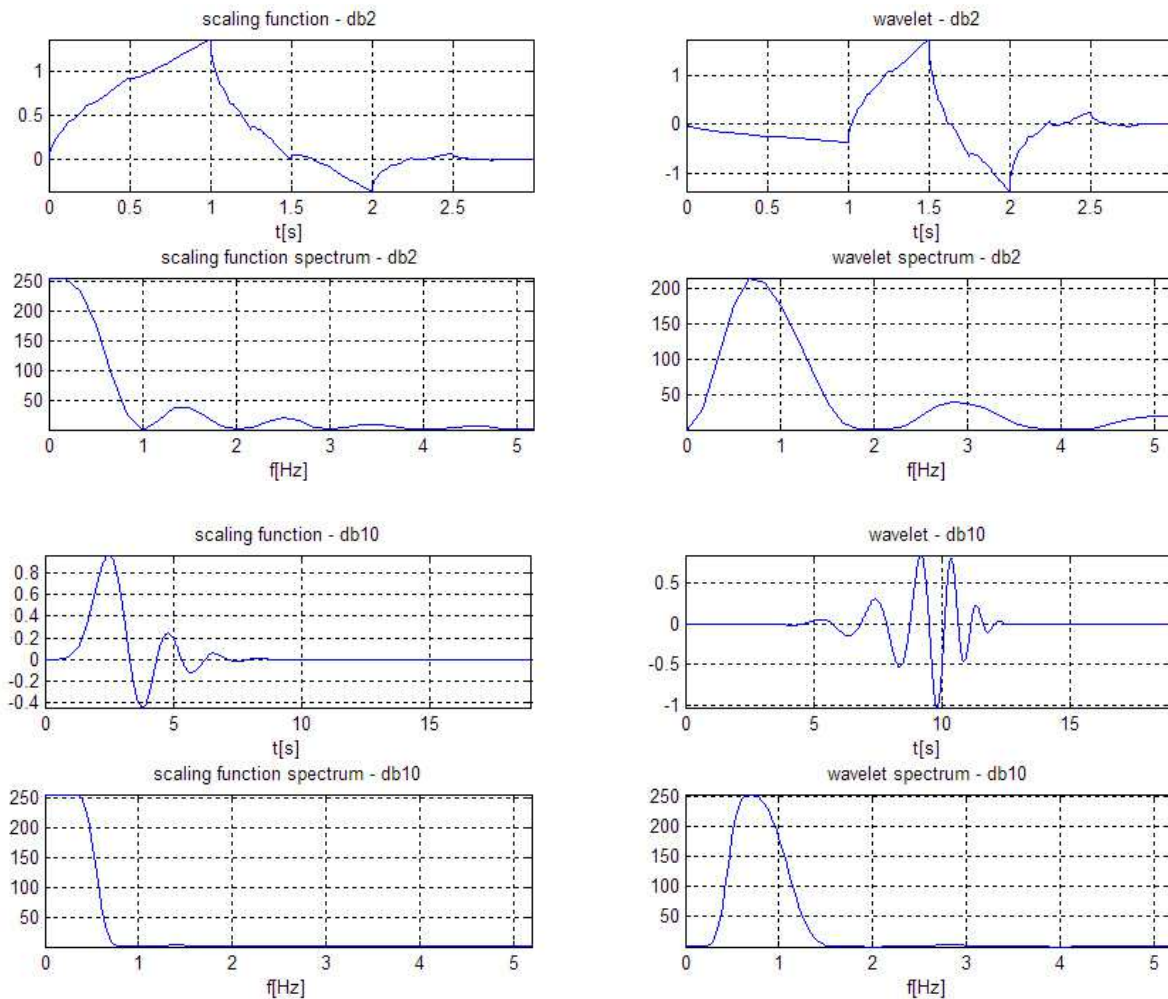


Fig. 11. Two examples of wavelets with scaling functions and their spectra (2<sup>nd</sup> order Daubechies – db2, 10<sup>th</sup> order Daubechies – db10).

Coiflets were also created by Ingrid Daubechies. They are also defined by a recursive formula and do not have an explicit description. If N is an order of a wavelet function  $\psi$ , the number of vanishing moments is equal to  $2N$ , while the number of vanishing moments of the scaling function  $\varphi$  is equal to  $2N-1$ . Coiflets have the operating range equal to  $6N-1$  and are much more symmetrical than Daubechies wavelets. They are also orthogonal.

The wavelet representation can be easily extended to the n-dimensional space ( $n > 1$ ). In practice, the two-dimensional space is in widespread use, for example for image processing. A special case of a two-dimensional multi-resolution approximation is the separable multi-resolution approximation. It has been shown that in this case the scaling function  $\varphi(x,y)$  can be written in the form  $\varphi(x,y) = \varphi(x)\varphi(y)$ , where  $\varphi(x)$  and  $\varphi(y)$  are one-dimensional scaling functions.

## 11. Applications of the time-frequency and wavelet analysis

In general, signal representations in time-frequency and time-scale domains are most often used in the vibro-acoustics, speech signal analysis, biomedical signal (ECG, EEG) analysis, power network analysis, pulse echography and telecommunications [22–24]. In vibro-acoustics the  $t/f$  analysis provides information on the level of noise and possible defects of machines. In the case of a speech signal, it gives the ability to recognize individual features of a speaker or even the content of speech. For biomedical signals, the  $t/f$  analysis enables detection of certain signal features useful in medical diagnosis. It must be remembered that the choice of the type of  $t/f$  representation can have a significant impact on the shape of the spectrum obtained and the possibility of its interpretation. Each representation has its own advantages and disadvantages in relation to a specific application [25, 26].

The  $t/f$  algorithms were implemented in - designed by the authors – a virtual instrument for the time-frequency analysis of an arbitrary one-dimensional signal. The virtual instrument consists of a PC, a data acquisition board (DAQ) and a LabWindows/CVI programming environment. Examined signals may be read directly by the DAQ board or from a file in ASCII format. Prior to the time-frequency analysis it is possible to remove a trend from the examined signal. This allows us to better visualize the spectrogram of a signal without a DC or low frequency trend.

The designed virtual instrument has been used to analyze the speech and biomedical signals, such as ECG and phonocardiograms. An example of the time-frequency analysis of a speech signal is presented in Fig. 12 and 13.

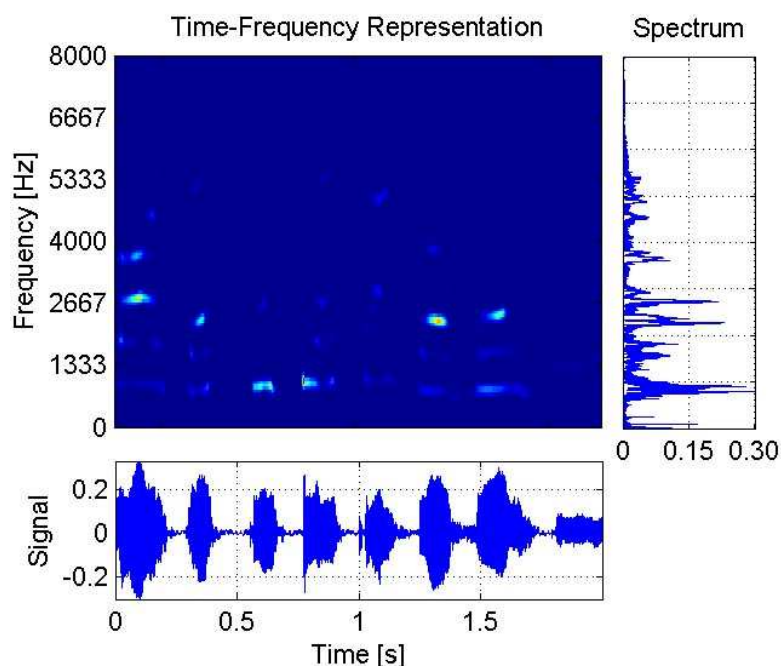


Fig. 12. The  $t/f$  decomposition of a speech signal – the linear scale.

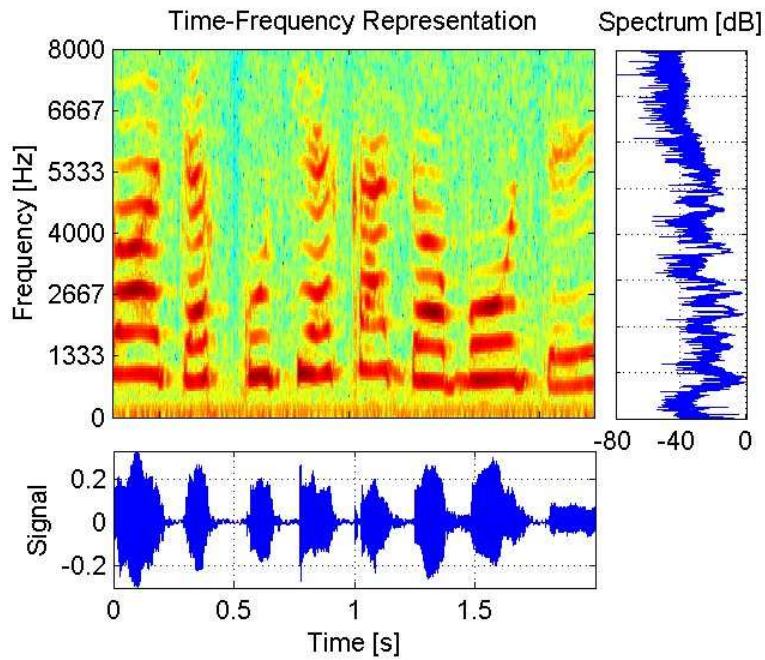


Fig. 13. The t/f decomposition of a speech signal – the logarithmic scale.

The spectrogram observation allows to illustrate the mechanism of human speech. The spectrogram presented in Fig. 12 shows the signal energy as a function of time and frequency in the linear scale. The diagram in the top right corner shows the power spectrum of the signal in the linear scale. It's obvious that it carries much less information than the spectrogram. The spectrogram plotted in the logarithmic scale (Fig. 13) enables to observe large differences between amplitudes of individual frequency components.

Another important application of the t/f analysis is evaluation of the power quality. The effect of analyzing a power network signal (50 Hz) disturbed with 700Hz oscillations is given in Fig. 14.

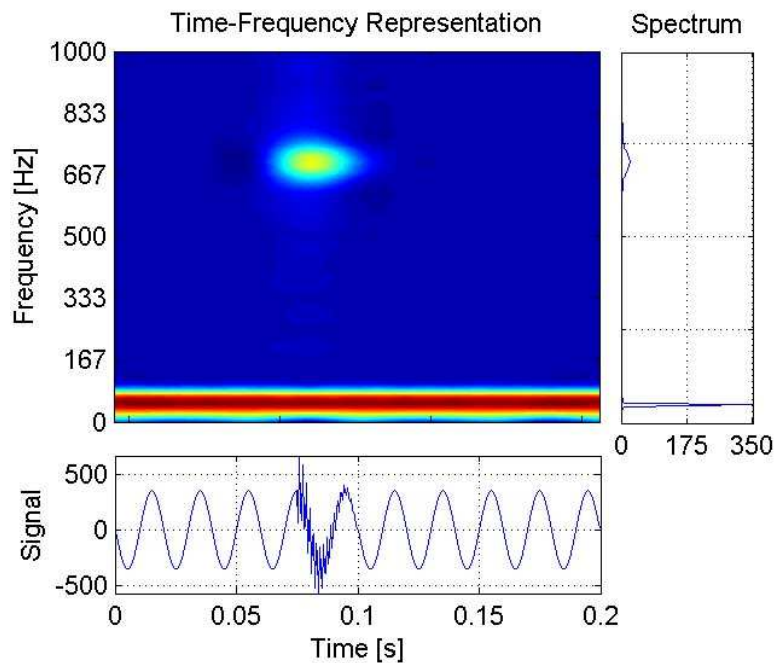


Fig. 14. The effect of analyzing a power network signal (50 Hz) disturbed with 700Hz oscillations.

The next example (Fig. 15) contains a disturbed (by breathing) ECG signal. The Daubechies wavelet of the 4th order and the five-level decomposition were used. The details reflect clearly extracted fragments of signal corresponding to the wavelet at the appropriate scale.

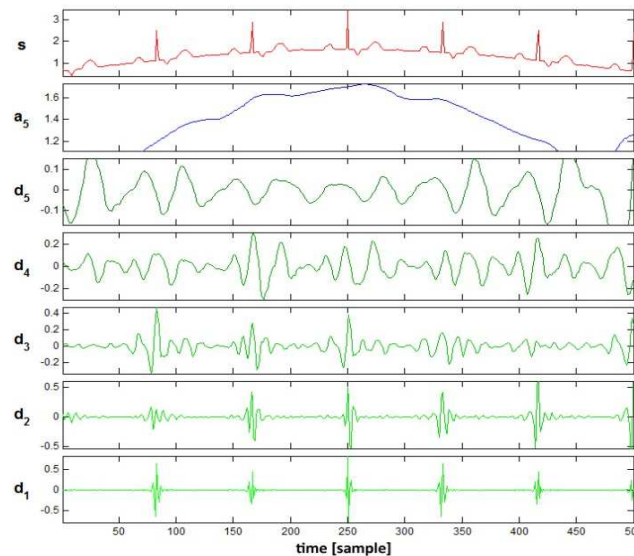


Fig. 15. The discrete wavelet transform analysis: the ECG signal (from the top: the signal, the approximation, the details in the scales of 5,4,3, 2 and 1).

In the case of an ECG, the most interesting results are observed in the scales 1 and 2. This type of analysis may be used to precisely determine the location of some characteristic points of an ECG (QRS) signal, which are important from the medical diagnosis point of view.

## 12. Summary

For purposes of the analysis of non-stationary signals, it is necessary to present the frequency characteristics as a function of time. Roughly, this is done by calculating the instantaneous signal spectra on the basis of its fragments, designated by observation of the time window, sliding along the signal. In general, time-frequency methods allow to explore the properties of the signal in the joint time and frequency domains. The family of time-frequency representations of non-stationary signals includes Short-Time Fourier transform, Gabor transform, Wigner-Ville, Choi-Williams, Cone-shaped, and many others.

Time-frequency methods of signal analysis are widely used in practice. The most popular is processing of speech signals, biomedical signals (EEG, ECG) [27], seismic signals and electrical power network signals [28]. The  $t/f$  analysis also plays a very important role in the vibration analysis of machine testing. The methods give a lot more interesting results than the use of a traditional spectral analysis. Very interesting effects may also be observed in the case of highly noisy signals. Even signals hidden under the background noise can leave clear marks in a spectrogram.

The wavelet analysis was originally designed as a tool that could eliminate the disadvantages of both traditional and Short-Time Fourier spectrum analysis. The goal was achieved: the  $t/f$  resolution changes over a single iteration of the analysis. Owing to that fact the wavelet analysis has an extremely wide range of applications. However, thinking that the only advances in the wavelet analysis include just refreshing and unification of already known theories and techniques is an ill-founded misconception. There are still vast ranges of new applications and discoveries in this field waiting to be made.

## References

- [1] Boashash, B. (2003). *Time–Frequency Signal Analysis and Processing: A Comprehensive Reference*. Elsevier Science, Oxford.
- [2] Time-Frequency Toolbox for use with MATLAB. (1996). CNRS (France) and Rice University (USA).
- [3] Mallat, S. (1989). A Theory of Multiresolution Signal Decomposition: The Wavelet Representation. *IEEE Transactions on Pattern Analysis and Machine Intelligence*, 7, 674–693.
- [4] Qian, S. (2002). *Introduction to Time-Frequency and Wavelet Transforms*, Prentice Hall Professional Technical Reference.
- [5] Mallat, S. (1998). *A wavelet Tour of Signal Processing*, Academic Press.
- [6] Boualem Boashash, B. (2003). *Time Frequency Analysis*. Gulf Professional Publishing.
- [7] Qian, S., Chen, D. (1999). Joint time-frequency analysis. *IEEE Signal Processing Magazine*, 2, 52–67.
- [8] Nievergelt, Y. (2013). *Wavelets Made Easy*, Springer.
- [9] Goswami, J. C., Chan, A. K. (1999). *Fundamentals of wavelets – Theory, Algorithms and Applications*. John Wiley & Sons Inc. New York.
- [10] Signal Processing Toolset User Manual. (2001). National Instruments.
- [11] Burrus, C. S., Gopinath, R. A., Guo, H. (1998). *Introduction to Wavelets and Wavelet Transforms: A Primer*. Prentice Hall Inc.
- [12] Qian, S., Chen, D. (1996). *Joint Time-Frequency Analysis*. Englewood Cliffs, N.J., Prentice-Hall.
- [13] Cohen, L. (1995). *Time–Frequency Analysis*. Prentice-Hall, New York.
- [14] Cohen, L., Loughlin, P. (1998). *Recent Developments in Time-Frequency Analysis*. Springer.
- [15] Heil, C., David, F., Walnut, D.F. (2000). *Fundamental Papers in Wavelet Theory*. Princeton University Press.
- [16] Meyer, Y., Ryan, R. D. (1993). *Wavelets: Algorithms & Applications*. Society for Industrial and Applied Mathematics.
- [17] Kaiser, G. (1999). *A Friendly Guide to Wavelets*. C. Valens.
- [18] Cohen, A. (2003). *Numerical Analysis of Wavelet Methods*. North Holland.
- [19] Van den Berg, J. C. (2004). *Wavelets in Physics*. Cambridge University Press.
- [20] Daubechies, I. (1992). *Ten Lectures on Wavelets*. Society for Industrial and Applied Mathematics.
- [21] Wavelet Toolbox for use with Matlab. (2012). Mathworks Inc.
- [22] Flandrin, P. (1999). *Time–frequency/Time–Scale Analysis, Wavelet Analysis and its Applications*, 10, Academic Press, San Diego.
- [23] Koornwinder, T. H. (1993). *Wavelets: An Elementary Treatment of Theory and Applications*. World Scientific.
- [24] Mecklenbräuker, W., Hlawatsch, F. (1997). *The Wigner distribution: theory and applications in signal processing*. Elsevier.
- [25] Papandreou-Suppappola, A. (2010). *Applications in Time-Frequency Signal Processing*. Taylor & Francis.
- [26] Zieliński, T. P. (2009). *Digital signal processing. From theory to implementations*. WKŁ.
- [27] Jaffard, S., Meyer, Y., Ryan, R. D. (2001). *Wavelets, Tools for Science and Technology*. Society for Industrial and Applied Mathematics.
- [28] Boualem Boashash, B. (1992). *Time-frequency signal analysis--methods and applications*. Longman Cheshire.